Relativistic predictions of polarization phenomena in exclusive proton-induced proton-knockout reactions

G. C. Hillhouse[1], T. Ishida[2,3], T. Noro[2] and B. I. S. van der Ventel[1]

[1]Department of Physics, University of Stellenbosch, Stellenbosch, South Africa

[2]Department of Physics, Kyushu University, Fukuoka, Japan

ABSTRACT

Whereas a nonrelativistic distorted wave model fails to quantitatively describe analyzing power data for exclusive proton-induced proton-knockout from the $3s_{1/2}$ state in ^{208}Pb at 202 MeV, the corresponding relativistic prediction provides a perfect description, thus suggesting that the Dirac equation is the more appropriate underlying dynamical equation. We check the consistency of this result by comparing predictions for both dynamical models to new high resolution data for $3s_{1/2}$ knockout in ^{208}Pb at a higher incident energy of 392 MeV.

I. INTRODUCTION

Recently we demonstrated that a relativistic distorted wave model, represented by the solid line in Fig. (1), provides a perfect description of the energy-sharing analyzing power data for exclusive proton knockout from the $3s_{1/2}$ state in ^{208}Pb at an incident energy of 202 MeV. The corresponding nonrelativistic prediction, indicated by the dashed line in Fig. (1), completely fails to describe the data despite exhaustive corrections including different kinematic prescriptions for the NN amplitudes, non-local corrections to the scattering wave functions, and density-dependent modifications to the free NN scattering amplitudes [1, 2]. On the other hand, both Dirac and Schrödinger-equation-based models provide an excellent description of the unpolarized energy-sharing cross section, thus highlighting the application of spin observables, such as the analyzing power, for discriminating between different dynamical effects in nuclear systems.

Before claiming with absolute certainty that the relativistic Dirac equation is indeed the appropriate underlying dynamical equation, it is essential to check the consistency of the 202 MeV result by considering $3s_{1/2}$ knockout at another incident energy. In particular, one needs to evaluate to which extent the relatively poor energy resolution (310 KeV at

[3] Present address: Laboratory of Nuclear Science, Tohoku University, Sendai 982-0826, Japan.

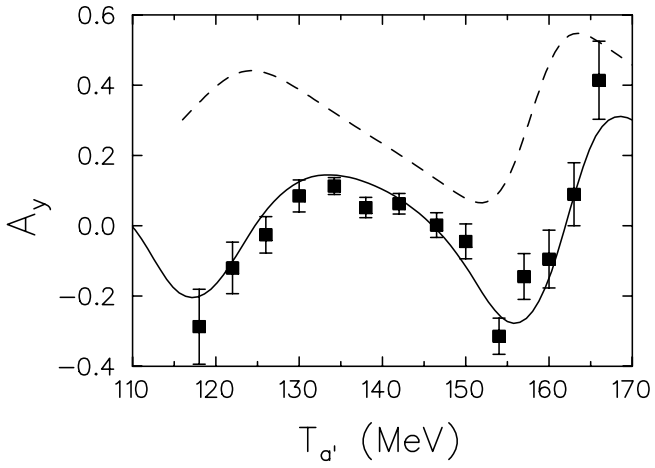

FIG. 1: Energy-sharing analyzing power A_y for the knockout of protons from the $3s_{1/2}$ state in ^{208}Pb, at an incident energy of 202 MeV, for coincident coplanar scattering angles ($\theta_{a'} = 28.0°$, $\theta_b = -54.6°$), plotted as a function of the kinetic energy of the proton scattered at angle $\theta_{a'}$. The dashed and solid curves represent the nonrelativistic and relativistic distorted wave predictions respectively. The data are from Ref. [1].

FWHM), and resulting offline peak fitting analysis associated with the 202 MeV data, influences the quality of $3s_{1/2}$ analyzing power data and interpretation thereof [1]. Indeed, the Kyushu University experimental nuclear physics group have recently performed a high resolution (250 KeV at FWHM) study of the $^{208}\mathrm{Pb}(\vec{p}, 2p)^{207}\mathrm{T}\ell$ reaction at an incident energy of 392 MeV at the Research Center for Nuclear Physics in Japan [3]: cross section and analyzing power data (energy-sharing and angular distributions) were measured for proton knockout from the $3s_{1/2}$-, $2d_{3/2}$, $2d_{5/2}$ and $1h_{11/2}$-states. A typical binding-energy spectrum is displayed in Fig. (2).

In this paper, we focus on the theoretical interpretation of the $3s_{1/2}$ cross section and analyzing power data at 392 MeV. In particular we compare both relativistic and nonrelativistic distorted wave predictions to these new data so as to confirm or refute the previous claim at 202 MeV that relativistic dynamics are essential for a correct description of the $3s_{1/2}$ analyzing power. Furthermore, we also identify additional independent polarization transfer observables which need to be measured to further study the role of relativity in nuclear reactions. Note that the original motivation for choosing a heavy target nucleus such as ^{208}Pb was to maximize the influence of the nuclear medium of the scattering wave functions, while still maintaining the validity of the impulse approximation, and also avoiding complications

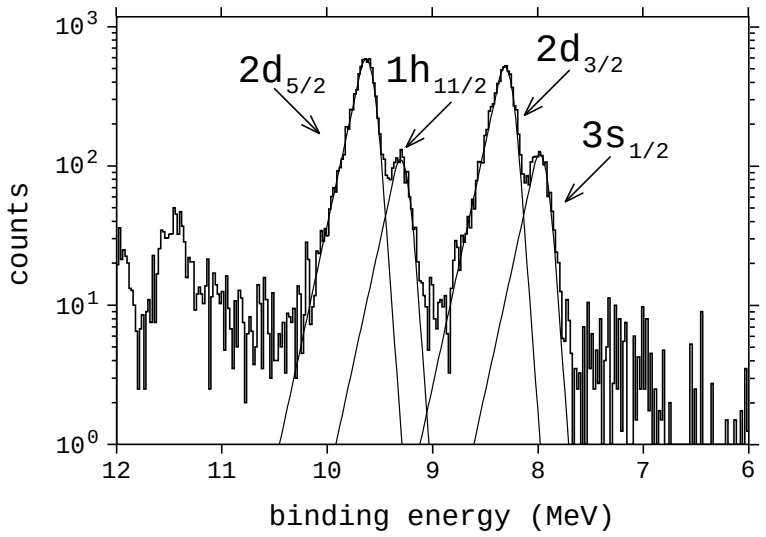

FIG. 2: A typical binding-energy spectrum for the ^{208}Pb$(\vec{p},2p)^{207}$Tℓ reaction at 392 MeV. The relevant single-particle proton-hole states in ^{208}Pb are indicated. The data are from Ref. [3].

associated with the inclusion of recoil corrections in the relativistic Dirac equation. In addition, for the knockout of $3s_{1/2}$ valence protons one expects density-dependent corrections to the NN interaction to be negligible.

This paper is organized as follows: we briefly review the main aspects of the relativistic and nonrelativistic distorted wave models in Secs. (II) and (III) respectively. The relevant scattering observables are defined in Sec. (IV), and results and conclusions are presented in Sec. (V).

II. RELATIVISTIC MODEL

The formalism for the relativistic distorted wave model has been presented in Refs. [2, 4–7]. In this paper we briefly allude to the most important aspects of the model and refer the interested reader to the latter references for more detail.

The exclusive $(p,2p)$ reaction of interest is schematically depicted in Fig. (3), whereby an incident proton, a, knocks out a bound proton, b, from a specific orbital in the target nucleus A, resulting in three particles in the final state, namely the recoil residual nucleus, C, and two outgoing protons, a' and b, which are detected in coincidence at coplanar laboratory scattering angles, $\theta_{a'}$ and θ_b, respectively. All kinematic quantities are completely determined by specifying the rest masses, m_i, of particles, where $i = (a,A,\, a',\, b,\, C)$, the laboratory kinetic

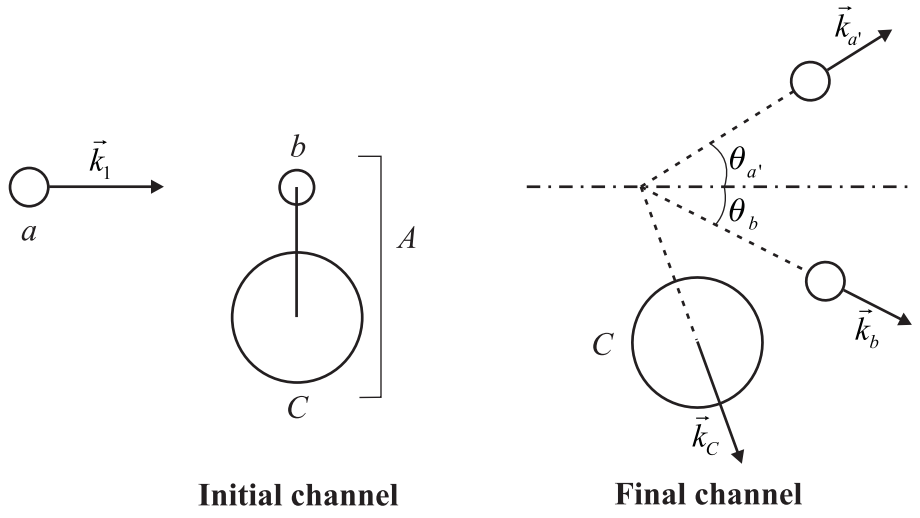

FIG. 3: Schematic representation for the coplanar $(p, 2p)$ reaction of interest.

energy, T_a, of incident particle a, the laboratory kinetic energy, $T_{a'}$, of scattered particle a', the laboratory scattering angles $\theta_{a'}$ and θ_b, and also the excitation energy of the proton that is to be knocked out of the target nucleus, A.

We adopt a zero-range approximation to the NN interaction, whereby the relativistic distorted wave transition matrix element is given by

$$T_{LJM_J}(s_a, s_{a'}, s_b) = \int d\vec{r}\,[\,\bar{\Psi}^{(-)}(\vec{r}, \vec{k}_{a'C}, s_{a'}) \otimes \bar{\Psi}^{(-)}(\vec{r}, \vec{k}_{bC}, s_b)\,] \hat{F}_{NN}(T_{\rm eff}^{\ell \rm ab}, \theta_{\rm eff}^{\rm cm})\,[\,\Psi^{(+)}(\vec{r}, \vec{k}_{aA}, s_a) \otimes \Phi^B_{LJM_J}(\vec{r})\,] \quad (1)$$

where $\otimes$ denotes a Kronecker product. The four-component scattering wave functions, $\psi(\vec{r}, \vec{k}_i, s_i)$, are solutions to the fixed-energy Dirac equation with spherical scalar and time-like vector nuclear optical potentials: $\Psi^{(+)}(\vec{r}, \vec{k}_{aA}, s_a)$ is the relativistic scattering wave function of the incident particle, a, with outgoing boundary conditions [indicated by the superscript $(+)$], where $\vec{k}_{aA}$ is the momentum of particle a in the $(a + A)$ center-of-mass system, and s_a is the spin projection of particle a with respect to $\vec{k}_{aA}$ as the $\hat{z}$-quantization axis; $\bar{\Psi}^{(-)}(\vec{r}, \vec{k}_{jC}, s_j)$ is the adjoint relativistic scattering wave function for particle j [$j = (a', b)$] with incoming boundary conditions [indicated by the superscript $(-)$], where $\vec{k}_{jC}$ is the momentum of particle j in the $(j + C)$ center-of-mass system, and s_j is the spin projection of particle j with respect to $\vec{k}_{jC}$ as the $\hat{z}$-quantization axis. We employ a global scalar and vector Dirac optical potential parameter set for the distorting optical potentials. More specifically, we use the energy-dependent mass-independent "EDAI-fit" parameter set

which has been constrained by proton elastic scattering data on ^{208}Pb for incident proton energies between 21 MeV and 1040 MeV [8]. The four-component relativistic boundstate proton wave function, which is denoted by $\Phi^B_{LJM_J}(\vec{r})$ in Eq. (1) and labeled by single-particle quantum numbers L, J, and M_J, is obtained via selfconsistent solution to the Dirac-Hartree field equations within the context of the relativistic mean field approximation associated with the QHDII Lagrangian density [9] of quantum hadrodynamics [10]. We also employ the impulse approximation which assumes that the form of the NN scattering matrix in the nuclear medium is the same as that for free NN scattering. In addition, we adopt the IA1 representation [11] which parameterizes the NN scattering matrix $\hat{F}_{NN}(T^{\ell\rm ab}_{\rm eff}, \theta^{\rm cm}_{\rm eff})$ in terms of five Lorentz invariant amplitudes (scalar, pseudoscalar, vector, axial-vector, tensor) which are directly related to the five nonrelativistic Wolfenstein amplitudes describing on-shell NN experimental scattering data: $T^{\ell\rm ab}_{\rm eff}$ and $\theta^{\rm cm}_{\rm eff}$ represent the effective two-body laboratory kinetic energy and center-of-mass scattering angles, respectively, based on the so-called final-energy prescription [12].

III. NONRELATIVISTIC MODEL

All of the nonrelativistic calculations are based on the computer code THREEDEE of Chant and Roos [12], where the nonrelativistic transition amplitude, based on a zero-range approximation to the NN interaction, is

$$T^{\rm NRDW}_{LJM_J}(s_a, s_{a'}, s_b) = \int d\vec{r}\,[\,\psi^{*(-)}(\vec{r}, \vec{k}_{a'C}, s_{a'}) \otimes \psi^{*(-)}(\vec{r}, \vec{k}_{bC}, s_b)\,] \\ \hat{t}_{NN}(T^{\ell\rm ab}_{\rm eff}, \theta^{\rm cm}_{\rm eff})[\,\psi^{(+)}(\gamma\vec{r}, \vec{k}_{aA}, s_a) \otimes \varphi^B_{LJM_J}(\vec{r})\,], \qquad (2)$$

where the ψ's represent the appropriate incoming and outgoing nonrelativistic two-component scattering wave functions and φ is the nonrelativistic wave function of the bound proton to be knocked out, and $\gamma = A/(A+1)$, where A being the target mass number: both scattering and boundstate wave functions are solutions to the Schrödinger equation. For consistency between the relativistic and non-relativistic calculations, the nonrelativistic radial boundstate wave function is approximated by taking the upper component radial wave function of the relativistic four component boundstate wave function employed in the relativistic predictions. The scattering wave functions are solutions to the nonrelativistic Schrödinger equation employinga Schrödinger-equivalent representation [8] of the relativistic global opti-

cal potentials mentioned in Sec. (II). I n this paper we employ experimental amplitudes for the NN scattering matrix $\hat{t}_{NN}$ which are determined from the NN Arndt phase shift analysis (January 1999) [13]: these amplitudes are directly related to the relativistic Lorentz invariant amplitudes [11].

IV. SCATTERING OBSERVABLES

The spin observables of interest are denoted by $\mathrm{D}_{i'j}$ and are related to the probability that an incident beam of particles a with spin-polarization j induces a spin-polarization i' for the scattered beam of particles a': the subscript $j = (0, \ell, n, s)$ is used to specify the polarization of the incident beam, a, along any of the orthogonal directions

$$\hat{\ell} \;=\; \hat{z} \;=\; \hat{k}_{aA}\,, \quad \hat{n} \;=\; \hat{y} \;=\; \hat{k}_{aA} \times \hat{k}_{a'C}\,, \quad \hat{s} \;=\; \hat{x} \;=\; \hat{n} \times \hat{\ell}\,, \tag{3}$$

and the subscript $i' = (0, \ell', n', s')$ denotes the polarization of the scattered beam, a', along any of the orthogonal directions:

$$\hat{\ell}' \;=\; \hat{z}' \;=\; \hat{k}_{a'C}\,, \quad \hat{n}' \;=\; \hat{n} \;=\; \hat{y}\,, \quad \hat{s}' \;=\; \hat{x}' \;=\; \hat{n} \times \hat{\ell}'\,. \tag{4}$$

The choice $j\,(i') = 0$ is used to denote an unpolarized incident (scattered) beam. With the above coordinate axes in the initial and final channels, the spin observables, $\mathrm{D}_{i'j}$, are defined by

$$\mathrm{D}_{i'j} \;=\; \frac{\sum_{M_J, s_b} \mathrm{Tr}(T \sigma_j T^\dagger \sigma_{i'})}{\sum_{M_J, s_b} \mathrm{Tr}(T T^\dagger)}\,, \tag{5}$$

where $\mathrm{D}_{n0} = \mathrm{P}$ refers to the induced polarization, $\mathrm{D}_{0n} = \mathrm{A}_y$ denotes the analyzing power, and the other polarization transfer observables of interest are D_{nn}, $\mathrm{D}_{s's}$, $\mathrm{D}_{\ell'\ell}$, $\mathrm{D}_{s'\ell}$, and $\mathrm{D}_{\ell's}$. The denominator of Eq. (5) is related to the unpolarized triple differential cross section, i.e.,

$$\sigma \;=\; \frac{d^3\sigma}{dT_{a'}\, d\Omega_{a'}\, d\Omega_b} \;=\; S_{LJ}\, \sigma_{\mathrm{calc}}\,, \tag{6}$$

$$\sigma_{\mathrm{calc}} \;=\; \frac{F_{\mathrm{kin}}}{(2s_a + 1)\,(2J + 1)} \sum_{M_J, s_b} \mathrm{Tr}(T\, T^\dagger) \tag{7}$$

where F_{kin} is a kinematic factor and S_{LJ} is the spectroscopic factor [5, 6]. In Eq. (5), the symbols $\sigma_{i'}$ and σ_j denote the usual 2×2 Pauli spin matrices, and the 2×2 matrix T is given by

$$T \;=\; \begin{pmatrix} T_{LJ}^{s_a = +\frac{1}{2}, s_{a'} = +\frac{1}{2}} & T_{LJ}^{s_a = -\frac{1}{2}, s_{a'} = +\frac{1}{2}} \\ T_{LJ}^{s_a = +\frac{1}{2}, s_{a'} = -\frac{1}{2}} & T_{LJ}^{s_a = -\frac{1}{2}, s_{a'} = -\frac{1}{2}} \end{pmatrix} \tag{8}$$

where $s_a = \pm\frac{1}{2}$ and $s_{a'} = \pm\frac{1}{2}$ refer to the spin projections of particles a and a' along the $\hat{z}$ and $\hat{z}'$ axes, defined in Eqs. (3) and (4), respectively; the matrix $T_{LJ}^{s_a,s_{a'}}$ is related to the relativistic $(p,2p)$ transition matrix element $T_{LJM_J}(s_a, s_{a'}, s_b)$, defined in Eq. (1) via

$$T_{LJ}^{s_a,s_{a'}} \;=\; T_{LJM_J}(s_a, s_{a'}, s_b)\,. \tag{9}$$

V. RESULTS AND CONCLUSIONS

The experimental data (experiment E205) were measured using the dual-arm spectrometer at RCNP [3]. For a direct comparison to data both relativistic (RDWIA)and nonrelativistic (NRDWIA) distorted wave predictions were corrected (using a Monte-Carlo simulation) for the finite angle acceptance of both Grand Raiden and the Large Acceptance Spectrometers: note that the current version of the relativistic code does not consider out-of-plane predictions, and consequently the RDWIA calculations exclude finite azimuthal angle ϕ corrections to the solid angle.

We now compare theoretical RDWIA and NRDWIA energy-sharing and angular distribution predictions of cross sections σ and analyzing powers A_y to experimental data for $3s_{1/2}$ knockout from ^{208}Pb at 392 MeV. In Fig. (4) the energy-sharing distributions (left panel) are plotted as a function of the kinetic energy $T_{a'}$ for coincident coplanar laboratory scattering angles (32.5°, -50.0°), and the angular distributions (right panel) are plotted as a function of the scattering angle θ_b, for $T_{a'} = 250$ MeV and $\theta_{a'} = 32.5^\circ$. Both RDWIA (solid curves) and NRDWIA (dashed curves) models provide a satisfactory description of the shape of the unpolarized cross sections for both energy-sharing and angular distributions. The analysis regarding the extraction of spectroscopic factors S_{LJ} and corresponding error bars is currently in progress: the values of S_{LJ} represent single-particle state occupation numbers and are obtained by normalizing the calculated cross sections σ_{calc} [see Eq. (7)] to the experimental cross section data.

Next we turn our attention to the analyzing power. As is the case for the 202 MeV data, the RDWIA energy-sharing distribution, indicated by the solid line in Fig. (4), is significantly reduced compared to the corresponding NRDWIA calculations (dashed line). Furthermore, the RDWIA prediction provides a better overall quantitative description of the data. Recall that for the 202 MeV data the energy-sharing analyzing power distribution for RDWIA was consistently reduced compared to the RDWIA calculations for all values of

$T_{a'}$. The latter is also true at 392 MeV, except at the maximum value of the cross section (at $T_{a'} \approx 245$ MeV) where both RDWIA and NRDWIA describe the data equally well. The RDWIA angular distribution is also consistently reduced compared to the NRDWIA result, except at $\theta_b \approx 50^\circ$ (corresponding to the maximum value of the cross section) where both models descrribe the data equally well. Hence, in general we conclude that at both 202 and 392 MeV, the RDWIA model is superior compared to the NRDWIA model, thus suggesting that relativistic dynamics are important for for describing $(p, 2p)$ reactions.

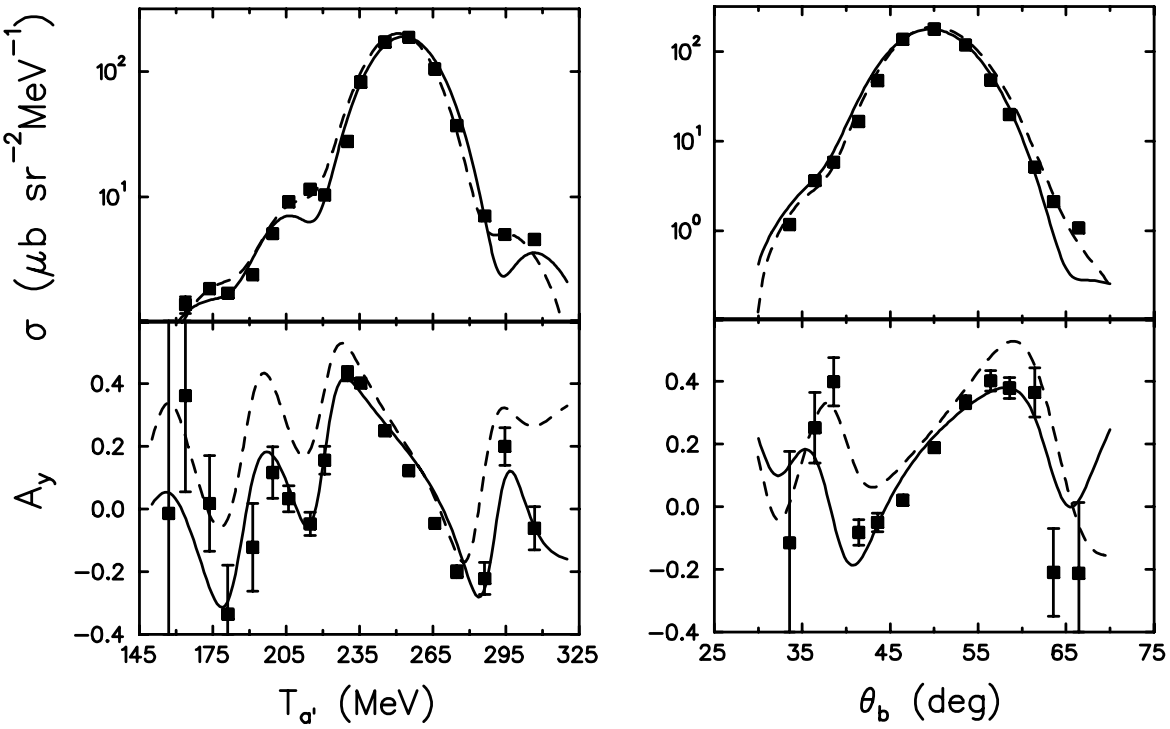

FIG. 4: Unpolarized triple differential cross section σ and analyzing power A_y for proton knockout from the $3s_{1/2}$ state in ^{208}Pb at an incident energy of 392 MeV plotted as a function of the kinetic energy $T_{a'}$ for coincident coplanar laboratory scattering angles (32.5°, −50.0°) (left panel), and as a function of the scattering angle θ_b, for $T_{a'} = 250$ MeV and $\theta_{a'} = 32.5^\circ$ (right panel). The dashed and solid curves represent the nonrelativistic and relativistic distorted wave predictions respectively. The data are from Ref. [3].

It is desirable to check the consistency of this result by also measuring other polarization observables which are sensitive to differences between relativistic versus nonrelativistic dynamical models. Based on the same kinematic conditions as for the 392 MeV analyzing power, we also identify the spin observables, D_{nn}, $D_{s's}$ and $D_{\ell'\ell}$ as good candidates for fur-

ther studying the role of relativity in nuclei: see Fig. (5): Other spin observables are not displayed since they are less sensitive to different dynamical effect.

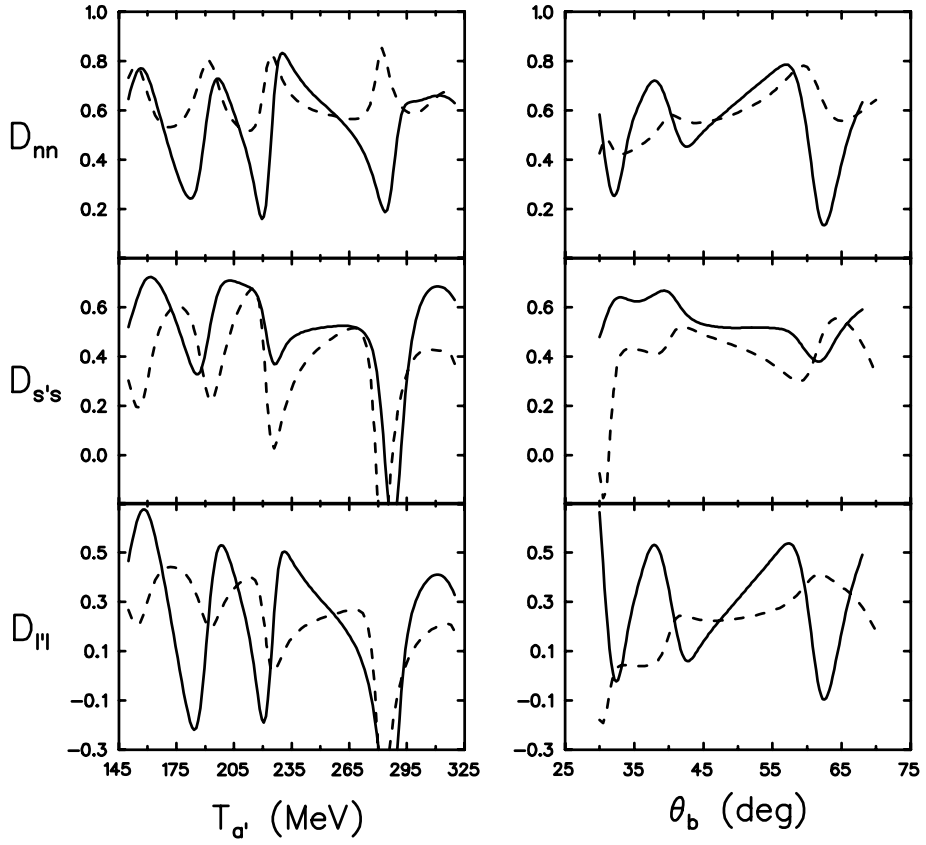

FIG. 5: Polarization transfer observables, D_{nn}, $D_{s's}$ and $D_{\ell'\ell}$, plotted as a function of either $T_{a'}$ (left panel) or θ_b (right panel) for kinematics corresponding to observables plotted in the left and right panels of Fig. (4) respectively. The dashed and solid curves represent the nonrelativistic and relativistic distorted wave predictions respectively.

The success of the RDWIA model to describe the knockout of the $3s_{1/2}$ valence nucleons in ^{208}Pb inspires confidence to extend our model to systematically address the topical question of how the free NN interaction is modified by the presence of the neighbouring nucleons in nuclei: the exclusive nature of $(p, 2p)$ reactions allows one to selectively knockout protons from deep- to low-lying single-particle orbitals in nuclei, thus enabling one to systematically study the effect of the nuclear density on the NN interaction. In addition, we intend to apply our RDWIA model to study exclusive proton knockout reactions from proton-rich and neutron-rich exotic nuclei using inverse kinematics at future radioactive beam facilities such as RIKEN and GSI. A drawback of the current implementation of the RDWIA model

is the use of the ambiguous IA1 parameterization for the NN scattering matrix. Future work will include study the effect of replacing the IA1 with the unambiguous IA2 representation in terms of 44 independent invariant amplitudes (of which the IA1 representation is a subset) which are consistent with parity and time-reversal invariance as well as charge symmetry [14].

Acknowledgments

We acknowledge support from the South African National Research Foundation under grant numbers 2054166 (GCH) and 2948567 (BISvdV). GCH also acknowledges support from the Japan Society for the Promotion of Science (GCH).

---

[1] R. Neveling, A. A. Cowley, G. F. Steyn, S. V. Förtsch, G. C. Hillhouse, J. Mano and S. M. Wyngaardt, Phys. Rev. C **66**, 034602 (2002).

[2] G. C. Hillhouse, J. Mano, A. A. Cowley, and R. Neveling, Phys. Rev. C **67**, 064604 (2003).

[3] T. Ishida, *Experimental study of a relativistic effect via the* $^{208}Pb(\vec{p},2p)^{207}Tl$ *reaction at 392 MeV* , Ph.D Thesis, Kyushu University (2006), unpublished.

[4] Y. Ikebata, Phys. Rev. C **52**, 890 (1995).

[5] O. V. Maxwell and E. D. Cooper, Nucl. Phys. **A603**, 441 (1996).

[6] J. Mano and Y. Kudo, Prog. Theor. Phys. Vol. 100, 91 (1998).

[7] G. C. Hillhouse, J. Mano, S. M. Wyngaardt, B. I. S van der Ventel, T. Noro, and K. Hatanaka, Phys. Rev. C **68**, 034608 (2003).

[8] E. D. Cooper, S. Hama, B. C. Clark, and R. L. Mercer, Phys. Rev. C **47**, 297 (1993).

[9] C. J. Horowitz and B. D. Serot, Nucl. Phys. **A368**, 503 (1981).

[10] C. J. Horowitz, D. P. Murdock, and B. D. Serot, in *Computational Nuclear Physics I*, edited by K. Langanke, J. A. Maruhn, and S. E. Koonin (Springer–Verlag, Berlin, 1991), p. 129.

[11] J. A. McNeil, L. Ray, and S. J. Wallace, Phys. Rev. C **27**, 2123 (1983).

[12] B. S. Chant and P. G. Roos, Phys. Rev. C **27**, 1060 (1983).

[13] R. A. Arndt, I. I. Strakovsky and R. L. Workman, Phys. Rev. C **62**, 034005 (2000).

[14] J. A. Tjon and Stephen J. Wallace, Phys. Rev. C **35**, 280 (1987).